Zeitschrift: Helvetica Physica Acta
Band: 55 (1982)
Heft: 6

Artikel: Scanning tunneling microscopy
Autor: Binnig, G. / Rohrer, H.
DOI: https://doi.org/10.5169/seals-115309

Helvetica Physica Acta, Vol. 55 (1982) 726–735 0018–0238/82/060726–10$1.50 + 0.20/0

Scanning tunneling microscopy

By G. Binnig and H. Rohrer, IBM Zurich Research Laboratory, CH-8803 Rüschlikon, Switzerland

(30. XII. 1982)

Abstract. Based on vacuum tunneling, a novel type of microscope, the scanning tunneling microscope (STM) was developed. It has an unprecedented resolution in real space on an atomic scale. We review the important technical features, illustrate the power of the STM for surface topographies and discuss its potential in other areas of science and technology.

1. Introduction

In the mid-fifties, Jörgen Olsen investigated the change of the shear modulus at the normal-superconducting transition [1]. This involved measurements of length changes of the order of 10^{-8}; at that time, quite a pioneering effort. It is therefore appropriate to present in this 'Festschrift' a new development which again ventures into small dimensions.

Towards the end of 1978, an investigation by the authors aimed at a better understanding of the growth, structure and the electrical properties of very thin oxide layers. The stimulus was given by statistical considerations of the influence of surface roughness on the performance of tunnel junctions [2], and experiments [3] supporting island-growth concepts [4] in thin oxide layers. To be able to make substantial progress in this field, it is necessary to observe structures and compositions of surfaces on an atomic scale. With no instrumentation available even approaching this requirement, we set out to develop our own instrument: the Scanning Tunneling Microscope (STM). As the name suggests, the STM is based on tunneling of electrons through an insulator, a physical effect known for more than 50 years [5] and widely exploited in science and technology. To use tunneling for the above investigations appeared obvious, but conventional tunneling with conductor-insulator-conductor sandwiches could not be achieved with atomic resolution, since these structures cannot yet be fabricated appreciably below the 1000 Å range. However, a sharp tip as one of the electrodes could provide the required resolution. GaAs tips had been used in tunnel studies of superconductors with the GaAs Schottky layer as tunnel barrier [6]. This method requires direct contact of tip and sample surface, and consequently damages the surface structure. Direct contact can be avoided when instead a vacuum gap serves as tunnel barrier [7]. Moreover, this has three distinct advantages. Firstly, the surface to be investigated is accessible at any time, both for treatment and other investigations. Secondly, vacuum is conceptually the simplest barrier, experimental data relate to the two electrodes alone. Thirdly, the tip can be moved freely over the surface, thus enabling scanning.

High resolution together with the scanning facility has now opened up fascinating possibilities in many areas of science and technology. Attempts to perform vacuum tunneling have so far been unsuccessful [8]. In the following, we first describe the technique of scanning tunneling microscopy [9, 10], the first application of spatially resolved vacuum tunneling, and review the crucial technical features making it feasible. Examples of STM graphs demonstrate the power of this method [9–11]. Finally, we present an outlook of the potential of scanning vacuum tunneling for other areas.

2. Principle of scanning tunneling microscopy

The operation of the STM is based on the strong distance dependence of a tunnel current, J_T. For two flat, parallel electrodes, J_T is given by [5]

$$J_T \propto (V_T/s) \cdot \exp(-A\phi^{1/2}s), \tag{2.1}$$

where $A \approx 1.025\,(\text{eV})^{-1/2}\,\text{Å}^{-1}$ for a vacuum gap, ϕ is the average of the two electrode work functions, s the distance between the electrodes, and V_T the applied voltage. With work functions of a few eV, J_T changes by an order of magnitude for every angstrom change of s. A schematic of the STM is shown in Fig. 1. The tunnel tip is fixed to a rectangular piezodrive P_x, P_y, P_z, made of commercial piezoceramic material. P_z and P_y scan the tip over the surface s. A voltage V_z is applied to the piezo P_z by the control unit CU such that the tunnel

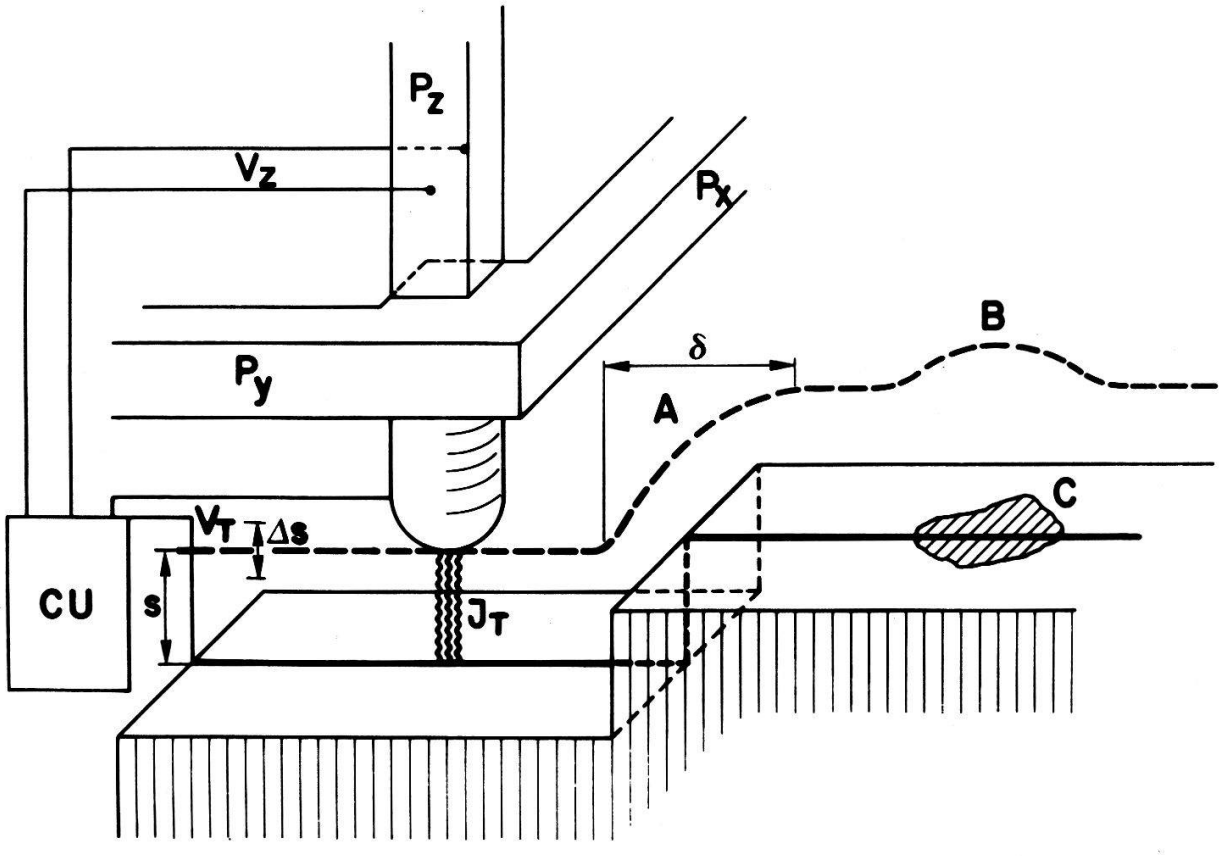

Figure 1
Principle of operation of the Scanning Tunneling Microscope (STM), explained in the text. © 1982 The American Physical Society.

current J_T remains constant. Thus, at *constant work function*, $V_z(V_x, V_y)$ gives the topography of the surface, $z(x, y)$, as illustrated at the surface step at A, i.e., the tunnel tip is moved at constant distance s over the surface. The value of s is usually unknown. By keeping the tunnel current constant, *changes in the work function* are compensated by corresponding changes in s. Thus, a lower work function at C induces the apparent surface structure B. Such induced structures, however, can be accounted for by measuring ϕ separately. The signal, $J_s = \Delta(\ln J_T)/\Delta s \approx \phi^{1/2}$, obtained by modulating the tunnel distance s by Δs while scanning, gives ϕ directly, at least in a simple situation as shown in Fig. 1. In general, separation of topography and work function is more involved, but still possible, since V_z and J_s contain ϕ and the topography in a different way.

3. Instrumental consideration

While the concept of the STM is quite simple, its realization encounters some delicate technical problems. Their solution was basic to the successful development of the STM. Considering that tip and sample have to be kept within a distance of about 10 Å with a stability of a tenth of an angstrom, it is obvious that the suppression of vibrations, both external ones and those created in the scanning and control process, was one central problem.

Suppression of external vibrations was initially achieved with superconducting magnetic levitation of the whole tunnel unit, combined with eddy-current damping. This gave very satisfactory results, but working at cryogenic temperatures in UHV is tedious, in particular in view of the continuous engineering improvements and changes required. At present, we use a two-stage spring system as shown in Fig. 2. This takes care of vibrations >1 Hz, except for high-frequency vibrations propagating along the springs themselves. These are damped out by Viton connectors mounted at each end of the spring [Fig. 3(a)]. The very thin electrical leads are led via Viton holders on the intermediate stage onto the tunnel unit and do not transmit any noticeable vibrations.

The second problem concerned the vibration-free approach of sample and tip. For mounting and certain treatments like sputter cleaning or flash desorption of contaminations, the sample has to be kept well away (say, up to millimeters) from the tip. Approaching the tip to within a convenient working range of the piezodrives of some 1000 Å had to be achieved without mechanical contact between the outside and the carefully protected tunnel unit. This rough drive, named the 'louse', is sketched in Fig. 3(b). Its body consists of a piezoplate (PP), with sample holder on top (not shown) and resting on three metal feet (MF), separated by high dielectric-constant insulators (I) from the metal groundplates (GP). The feet are clamped electrostatically to the groundplate by applying a voltage V_F. Elongating and contracting the piezobody of the louse with the appropriate clamping sequence of the feet moves the louse in any direction in steps between 100 Å to 1 μ and up to 30 steps/second.

The third vibration aspect deals with the operation of the STM itself. Both scanning and distance control are performed mechanically with the piezodrives. Thus, internally created vibrations cannot be avoided. However, they will not be detrimental if kept below the lowest mechanical eigenfrequencies of the tunnel unit, i.e., the cutoff frequency in the feedback loop CU for distance control has to

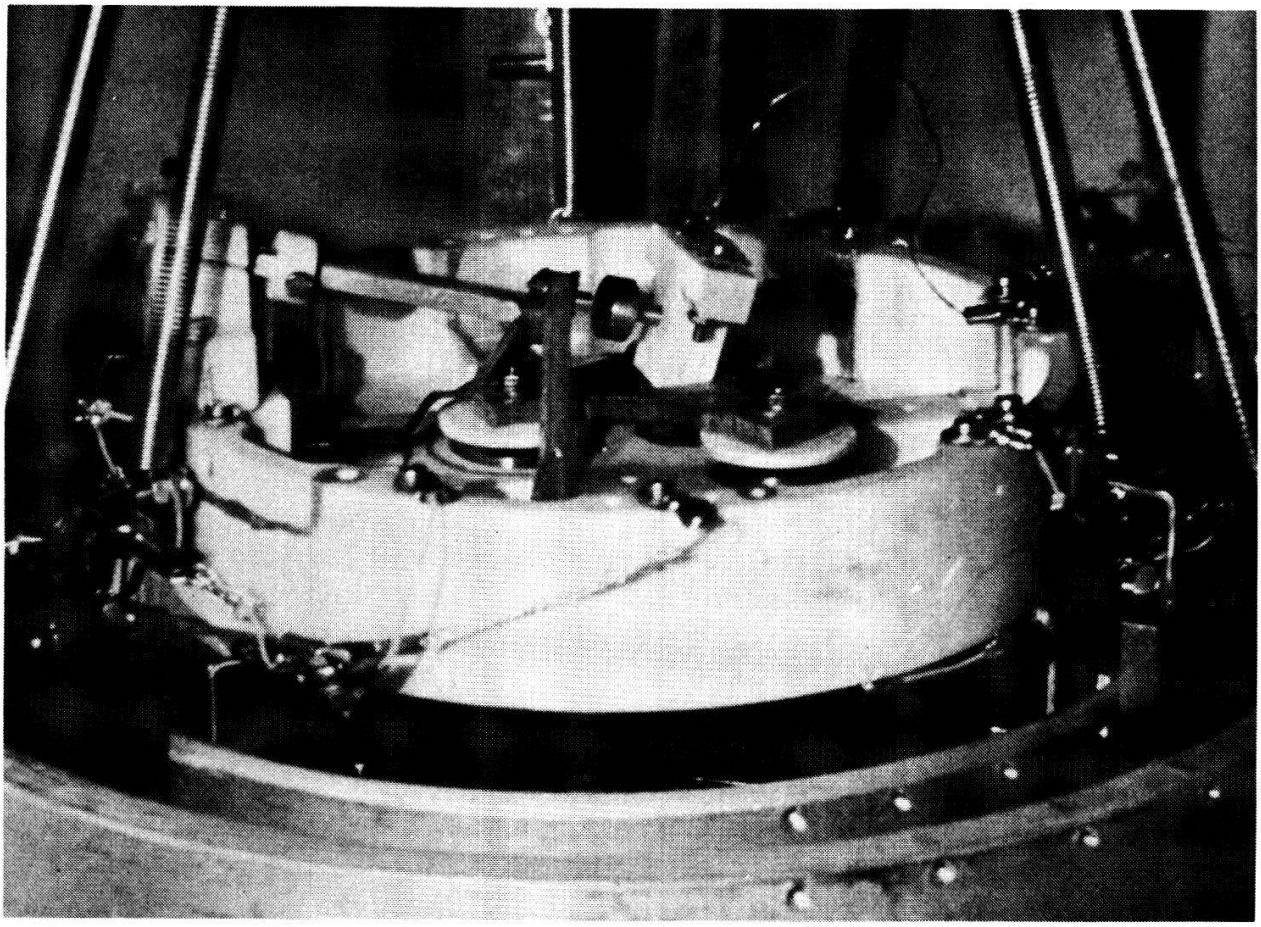

Figure 2
Tunnel unit showing piezodrives with tunnel-tip (left) and sample mounted on the 'louse' [see Fig. 3(b)]. © 1983 North-Holland.

be below this lowest mechanical resonance. For practical scanning speeds (say, a few hundred Å/sec), the latter have to lie above a few kHz. The crucial element in this respect was the piezodrive itself [see Fig. 3(c)]. The z-leg, P_z, of the rectangular piezodrive is rigidly fixed to P_z, P_y. Any displacement of the tunnel tip is due to elongation or bending of the three legs (each 4 cm long and 3 mm

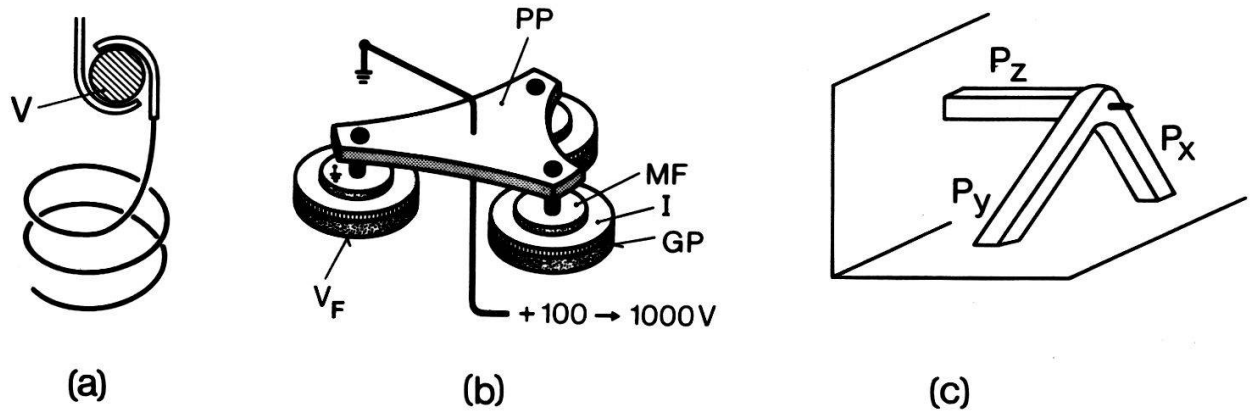

Figure 3
(a) High-frequency damping with Viton spacer, V. (b) Principle of 'louse'. (c) Rigid piezodrive with tunnel tip, all explained in the text.

quadratic cross-section). This results in a very rigid system with high eigenfrequency and linear elongation with applied voltages (elongations $\leq 10^{-4}$ cm).

The degree of vibration suppression determines the vertical resolution of the STM. The lateral resolution, on the other hand, is a matter of the sharpness of the tip. A very naive calculation for the resolution δ of a step (see Fig. 1) gives $\delta(\text{Å}) \approx 3\sqrt{R(\text{Å})}$, where R is the radius of curvature of the tip. A desired (and also achieved) resolution $\delta < 10$ Å would require $R \approx 10$ Å. This number does not appear very meaningful for a tip radius, but it is nevertheless clear that conventional field-emission tips ($R \approx 100$ to 1000 Å) would not provide the resolution desired. Although we do not yet understand the theoretical nor the detailed practical aspects of tunneling from such very pointed tips (a theory for tunneling from nonplanar small geometries is still lacking), we found a recipe to arrive at such resolutions. First, a Mo or W wire of about 1 mm diameter was ground at one end at roughly 90°. Scanning electron micrographs show overall tip radii of $<1\ \mu$ but the rough grinding process creates a few rather sharp minitips. The extreme sensitivity of the tunnel current on gap width then selects the minitip closest to the sample for tunneling. This yields a lateral resolution of about 20 Å. An advantage of these overall quite blunt tips is their much higher mechanical resonance frequencies than those of long and narrow field-emission tips. In-situ sharpening of the tip by gently touching the surface brings the resolution down to the 10 Å range, and the tips are quite stable. Finally, the resolution can still be increased considerably by exposing the tip for, say, half an hour, to electric fields of the order of 10^8 V/cm. We do not know whether this process extracts or migrates tip atoms, or adsorbs atoms on the tip. Unfortunately, these very sharp tips are not yet stable, and the very high resolutions cannot be maintained over longer periods. Reproducible fabrication of very sharp *stable* tips is one of the imminent engineering problems.

4. Surface topographies

The usual experimental methods to investigate surface structures (e.g., LEED, atom diffraction, ion channeling) are indirect in the sense that 'test models' are used to calculate the scattered intensity profile which is then compared with the one measured. In addition, these methods usually require periodic surface structures. The STM, on the other hand, gives 3d pictures of surface structures direct in real space, whether periodic or irregular. However, the STM graphs are not simply reproductions of surface-atom corrugation. They rather reflect the corrugation of the electron wave functions near the Fermi level, roughly in the middle of the vacuum gap. To make a quantitative connection with the corrugation of the surface cores, a detailed tunnel theory on the atomic scale is required, which, at present is still lacking although efforts in this direction are underway [12]. Nevertheless, we expect the STM graphs to qualitatively reflect the atomic surface structure. Figures 4 and 5 illustrate the power of scanning tunneling microscopy.

Figure 4 is an example of an irregular surface structure, exhibiting monoatomic $[\bar{2}11]$ steps on a Si(111) surface, up to 50 Å apart. The step lines are connected through angles of 60°. This is to be expected, if the steps are all of the same type. On the other hand, cleaved Si(111) surfaces exhibit only lines of $[2\bar{1}\bar{1}]$

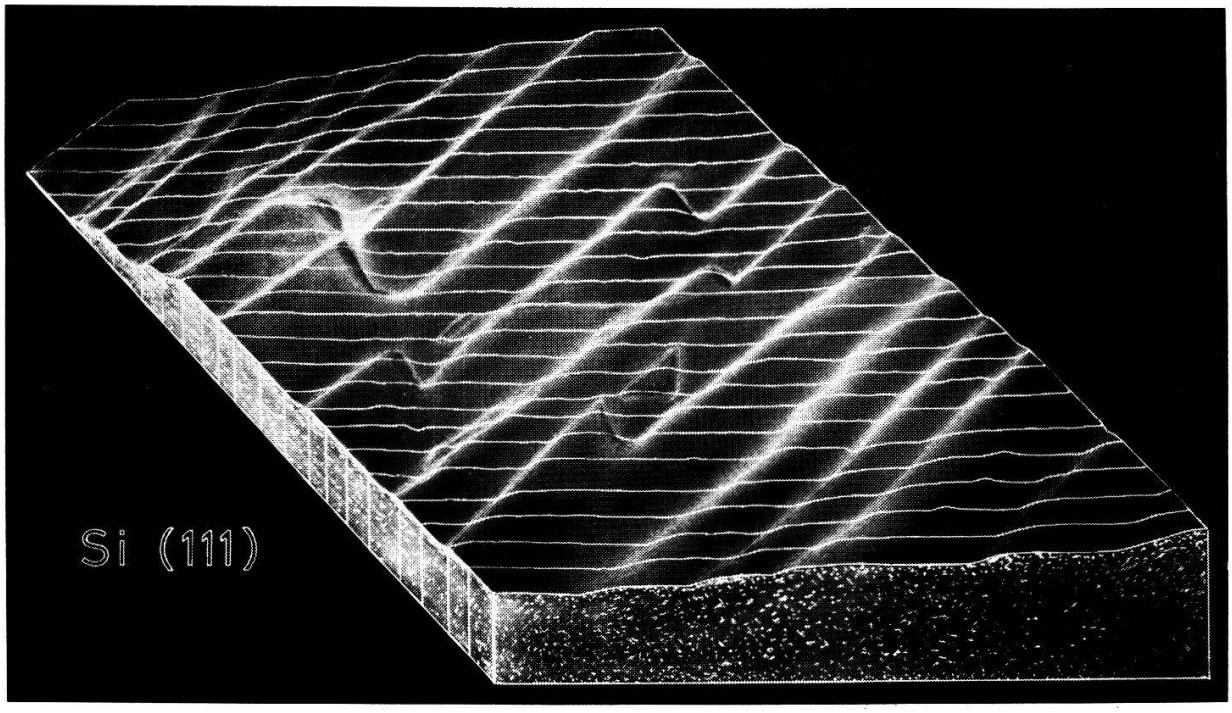

Figure 4
STM picture of a Si(111) surface exhibiting lines of mono-atomic step. © 1983 North-Holland.

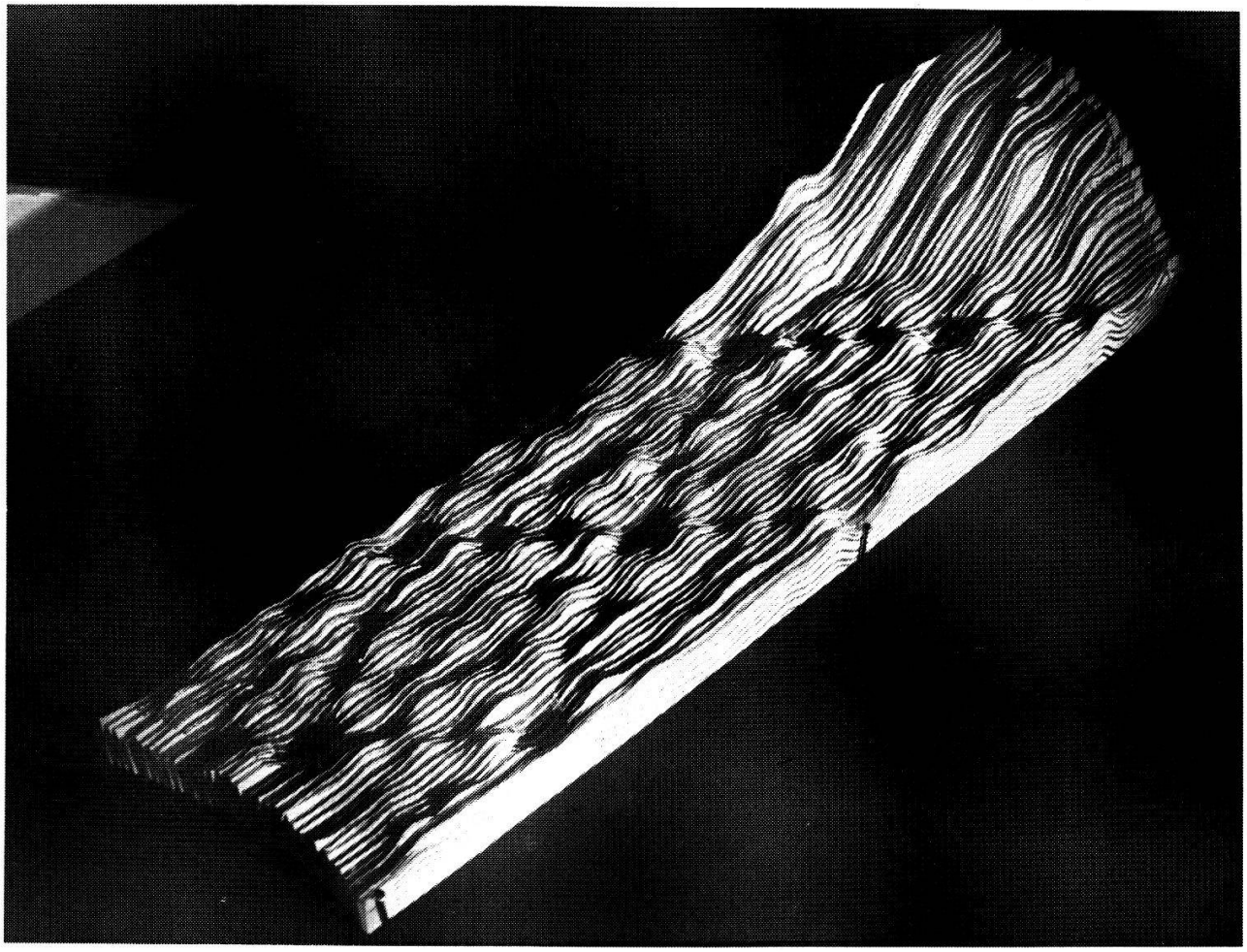

Figure 5
STM graph in relief form of the 7×7 reconstruction on Si(111), showing two complete rhombohedral unit cells. Deep minima (−2.1 Å) at the corners, minima (−0.9 Å) along the edges and 12 maxima (+0.7 Å) in the cell inside. © 1983 The American Physical Society.

steps, extending over many μ. Recent STM experiments even show that both types of step can occur on the same surface. This triggers a few interesting questions as to the influence of sample preparation and contamination on the surface structure of Si(111).

Figure 5 is at present our shining example of an STM graph, showing the famous 7×7 reconstruction of the Si(111) surface. This reconstruction has intrigued surface scientists for two decades. The original STM recordings in relief form show two complete rhombohedral 7×7 unit cells, clearly bounded by the lines of minima with deep corners. Inside each cell, 12 maxima appear. These are interpreted [11] as 12 Si adatoms, sitting on top of the Si(111) surface in distinct sites, and arranged in a unique manner. The different depth of the minima is attributed to an inhomogeneously relaxed top layer. Although a detailed interpretation of this surface structure still awaits both intensive calculations and a microscopic tunnel theory, we trust that this STM investigation is a decisive step towards clarifying the basic aspects of a long-standing intriguing problem. Moreover, it has demonstrated that scanning tunneling microscopy is able to clearly resolve individual atoms on a surface, less than 7 Å apart.

5. Resonant tunneling

Another, more academic example of the use of the STM is resonant tunneling. It also illustrates the simplest way to perform tunneling spectroscopy. Instead of measuring I–V characteristics requiring a new mode of operation, one can study $s-V$ (s is the tunnel distance) characteristics, remaining in the current stabilized mode.

Resonant tunneling is a consequence of matching wave functions. Consider the situation depicted in the inset of Fig. 6. When the applied voltage exceeds one of the work functions (in Fig. 6, $V>\phi_2$), the electron propagates as a free particle through part of the vacuum gap, after having crossed the triangular tunnel barrier. This is called field emission, and the tunnel current is a function of the electric field alone [13], (disregarding matching conditions),

$$J_T \propto E^2 \exp(-B/E). \tag{5.1}$$

Thus, for $J_T = \text{const}$, the gap width s is proportional to the applied voltage V. The right side of the vacuum gap then behaves like some sort of potential well, bounded on the left by the vacuum barrier and on the right by the metal surface. The latter is not strictly a potential barrier but acts as one in the sense that part of the wave is reflected due to the mis-match of the wave functions in the vacuum gap and in the metal. This reflection can be constructive or destructive depending on width and depth of the quasipotential well. In the case of constructive interference, the wave function in the well is enhanced, leading to a larger overlap in the barrier with the wave functions of the left metal electrode, and consequently to an increase of the tunnel current. Thus, J_T (at constant s), or in our case, s (at constant J_T) shows an oscillatory behavior as a function of V, superimposed on the form given by equation (5.1). In general, these oscillations cannot be observed with conventional tunnel junctions since the variation of the gap width has to be small compared to the wavelength at the right-side vacuum-metal interface, i.e., atomically flat electrode surfaces [14]. In Fig. 6, two $s-V$

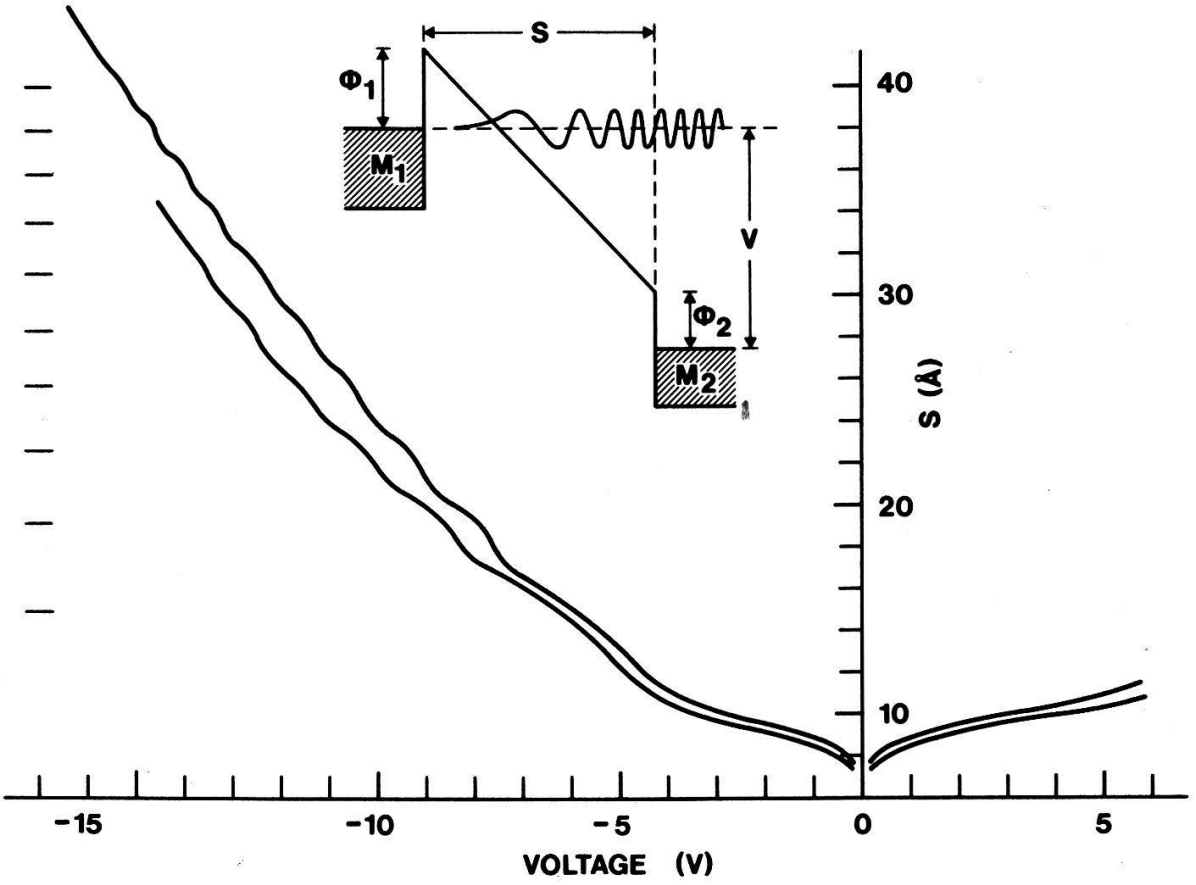

Figure 6
Distance-voltage tunnel characteristics exhibiting resonant tunneling. the 'levels' shown on the right are obtained from the resonance condition, equation (5.2), and give the distances for constructive interference. The inset shows schematically a metal (M_1)-vacuum-metal (M_2) tunnel junction under field-emission condition ($V > \phi_2$), and the propagating wave in the 'quasi-potential well' with corresponding decay in the triangular vacuum barrier (left) and the mismatch at the vacuum-M_2 interface.

characteristics are shown, taken on an atomatically flat part of an Au surface. For $V \ll \phi_2 \approx 5$ eV, the $s-V$ characteristic is given by equation (2.1), for $V > \phi_2$ it shows the linear relationship given by equation (5.1) with the oscillatory behavior superimposed. The oscillations agree well with those obtained from the resonance condition [15]

$$[(2n \pm 1/2)\alpha/0.203]^{2/3} = \mathrm{eV} - \phi_2, \tag{5.2}$$

where the + and − stand for maxima and minima of the oscillating part, and with $\alpha = (\phi_1 - \phi_2 + \mathrm{eV})/s$ and the absolute value of s determined from the field-emission part of the $s-V$ characteristic. The two curves have been taken with different tip geometries. Note that the field-emission region can only be reached with tip negative; reversed polarity always leads to instabilities, an interesting problem in itself.

6. Comparison with other microscopes

Figure 7, an up-dated version of the one given in [16], compares the resolution limits of various microscopes. It is probable that one or the other

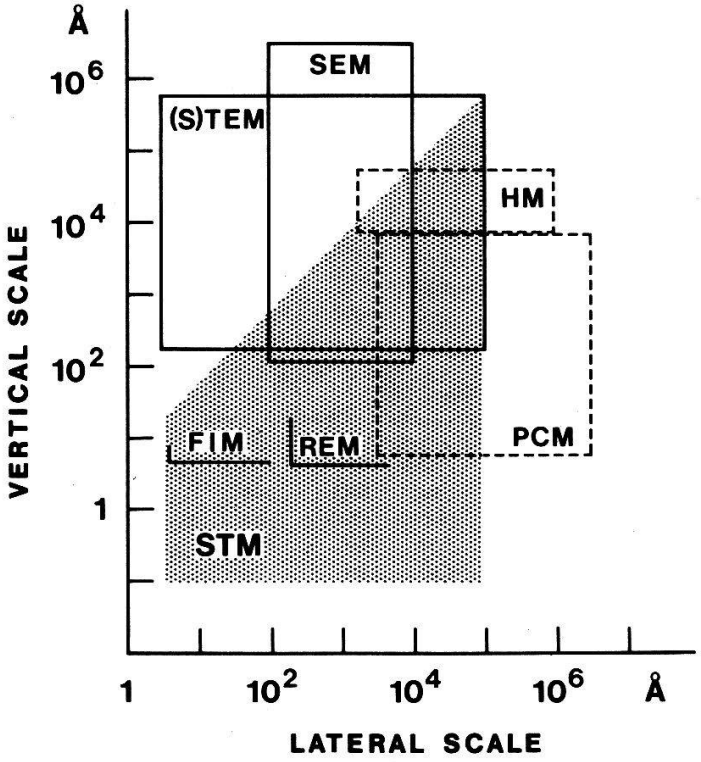

Figure 7
Comparison of resolutions of different microscopes. STM: shaded area. HM: high-resolution optical microscope, PCM: phase-contrast microscope, (S)TEM: (scanning) transmission electron microscope, SEM: scanning electron microscope, REM: reflection electron microscopé, and FIM: field ion microscope.

microscope can do better under very special circumstances. On the other hand, the top resolutions quoted already include special working conditions. Just to name a few: (a) very thin samples, underlying periodic structure, large mass contrast (e.g., heavy atom on carbon film) for the STEM and TEM; (b) strong corrugation or mass contrast for the SEM; (c) large atomically flat regions for the REM, and to some extent for the PCM; (d) tip geometry with only edge atoms of flat parts or adsorbate atoms on them visible, selected materials which are stable in high electric fields for the FIM. None of these requirements is necessary for the STM. Moreover, a very attractive feature of the STM is the high vertical *and* lateral resolution. It clearly shows that the STM does indeed advance into a new region. However, we should like to point out that we understand the STM as a complement to present microscopy rather than a competitor. For many applications, the STM is best used in combination with another microscope. An inherent limitation of the STM is that it always operates at high resolution. This sets a limit to the speed (decreased resolution does not mean high scanning speed, since the tunnel tip always has to follow the surface within tunnel distance).

7. Outlook

Surface topography is the first and simplest application of scanning tunneling microscopy. Experiments have so far dealt mainly with structures of clean

surfaces. Future developments of the technique will include mainly work-function profiles (for which encouraging results have already been obtained [9]) and tunneling spectroscopy, both with the same lateral atomic resolution as in the case of surface structures. This then opens the door to a great variety of interesting and topical problems like electronic properties of surfaces and surface states, structure of adsorbed molecules, preferential adsorption (e.g., preferential-adsorption sites and preferential orientation of adsorbates), growth, structure and electrical properties of thin insulating layers (the original aim of the STM), Schottky layers of clean and contaminated surfaces, and classical tunnel studies of materials for which sandwich-type tunnel junctions cannot be fabricated.

In many cases, the unique features of the STM are best brought to bear in combination with other supporting techniques, be it with other surface methods or other microscopes. Finally, considerable theoretical effort is still required, aimed at an understanding of microscopic tunneling and of concepts like work functions on an atomic scale. This will be an important factor for the evolution of scanning tunneling microscopy.

Acknowledgement

It is a pleasure for the authors to acknowledge the valuable contributions and continuous assistance of Ch. Gerber and W. Weibel and stimulating discussions with A. Baratoff, B. Reihl and K. H. Rieder.

REFERENCES

[1] J. L. Olsen, Nature *175* (1955) 37.
[2] A. Moser and K. E. Drangeid: private communication (1975).
[3] K. H. Rieder, Applications of Surf. Sci. *2* (1978) 74; *ibid. 4* (1980) 183.
[4] P. H. Holloway and J. B. Hudson, Surface Sci. *43* (1974) 123.
[5] R. H. Fowler and L. Nordheim, Proc. R. Soc. London *A119* (1928) 173; J. Frenkel, Phys. Rev. *36* (1930) 1604.
[6] S. von Molnar, W. A. Thompson and A. S. Edelstein, Appl. Phys. Lett. *11* (1967) 163; W. A. Thompson and S. von Molnar, J. Appl. Phys. *41* (1970) 5218; G. Guentherodt, W. A. Thompson, F. Holzberg and Z. Fisk, Phys. Rev. Lett. *49* (1982) 1030.
[7] G. Binnig, H. Rohrer, Ch. Gerber and E. Weibel, Appl. Phys. Lett. *40* (1982) 178; *ibid.* Physica *109 & 110B* (1982) 2075.
[8] I. Giaever, Rev. Mod. Phys. *46* (1974) 245; R. D. Young, J. Ward and F. Scire, Rev. Sci. Instrum. *43* (1972) 999; W. A. Thompson and S. F. Hanrahan, Rev. Sci. Instrum. *47* (1976) 1303.
[9] G. Binnig, H. Rohrer, Ch. Gerber and E. Weibel, Phys. Rev. Lett. *49* (1982) 57.
[10] G. Binnig and H. Rohrer, Surface Sci. (1983) in press.
[11] G. Binnig, H. Rohrer, Ch. Gerber and E. Weibel, Phys. Rev. Lett. *50* (1983) 120.
[12] A. Baratoff, *Third Europhysics Conference on Solid State Physics, Lausanne,* March 1983.
[13] J. G. Simmons, J. Appl. Phys. *34* (1963) 1793.
[14] J. Maserjian and N. Zamani, J. Appl. Phys. *53* (1982) 559; J. Maserjian, J. Vac. Sci. Technol. *11* (1974) 996.
[15] Equation (5.2) has been derived from the transfer Hamiltonian formalism, A. Baratoff: private communication; see also K. H. Gundlach, Solid-State Electron. *9* (1966) 949.
[16] H. Komatsu in *Crystal Growth and Characterization,* North Holland, 1975, p. 333.